The Asymmetrical Wind of the Candidate Luminous Blue Variable MWC 314

John P. Wisniewski[1], Brian L. Babler[2], Karen S. Bjorkman[3], Anatoly V. Kurchakov[4], Marilyn R. Meade[2], Anatoly S. Miroshnichenko[5]

ABSTRACT

We present the results of long-term spectropolarimetric and spectroscopic monitoring of MWC 314, a candidate Luminous Blue Variable star. We detect the first evidence of Hα variability in MWC 314, and find no apparent periodicity in this emission. The total R-band polarization is observed to vary between 2.21% and 3.00% at a position angle consistently around −0°, indicating the presence of a time-variable intrinsic polarization component, hence an asymmetrical circumstellar envelope. We find suggestive evidence that MWC 314's intrinsic polarization exhibits a wavelength-independent magnitude varying between 0.09% and 0.58% at a wavelength-independent position angle covering all four quadrants of the Stokes Q-U plane. Electron scattering off of density clumps in MWC 314's wind is considered as the probable mechanism responsible for these variations.

Subject headings: circumstellar matter stars: individual (MWC314) techniques: polarimetric techniques: spectroscopic

1. Introduction

As massive stars progress through the post-main-sequence evolutionary phase of their lifetimes, at least some will briefly enter the Luminous Blue Variable (LBV) evolutionary

[1]Universities Space Research Association/NASA GSFC Code 667, Building 21, Greenbelt, MD 20771, jwisnie@milkyway.gsfc.nasa.gov

[2]Space Astronomy Lab, University of Wisconsin-Madison, 1150 University Avenue, Madison, WI 53706

[3]Ritter Observatory, MS #113, Department of Physics and Astronomy, University of Toledo, Toledo, OH 43606

[4]Fesenkov Astrophysical Institute, 050020, Almaty Observatory, Kazakhstan

[5]Department of Physics & Astronomy, University of North Carolina-Greensboro, P.O. Box 26170, Greensboro, NC 27402

stage. Comprehensive reviews of LBVs and the properties of their circumstellar environments are given by Humphreys & Davidson (1994) and van Genderen (2001). Summarized briefly, LBVs are extremely luminous stars which exhibit photometric variability at multiple levels over a multitude of timescales, including large eruptions of up to 5 magnitudes on timescales of years to centuries, complex spectroscopic variability, and evidence of visible ejecta.

Only a limited number of LBVs or candidate LBVs (cLBVs) have been identified to date (e.g., van Genderen 2001), hindering efforts to understand the underlying physics which drive the variability of these objects. Miroshnichenko (1996) analyzed optical and near-IR photometry as well as optical spectroscopy of MWC 314 and concluded it was one of the most luminous stars in the Milky Way. While there is no record of MWC 314 undergoing a large photometric eruption and it doesn't show evidence of a dust shell, Miroshnichenko (1996) found MWC 314's fundamental parameters were similar to those of LBVs and thus suggested the object be classified as a cLBV. Followup high-resolution spectroscopy (Miroshnichenko et al. 1998) revealed MWC 314 had a N/O overabundance similar to that of other known LBVs; however, no evidence of spectral line variability was detected. These authors also suggested that MWC 314 possessed a non-spherical wind and that its circumstellar envelope was not oriented edge-on.

Polarimetry is well established as an effective tool to probe the geometry of circumstellar environments. Polarimetry has been utilized to investigate the environments of the LBVs AG Car (Leitherer et al. 1994; Schulte-Ladbeck et al. 1994; Davies et al. 2005), HR Car (Clampin et al. 1995; Parthasarathy et al. 2000; Davies et al. 2005), R127 (Schulte-Ladbeck et al. 1993), η Car (Schulte-Ladbeck et al. 1999; Davies et al. 2005), P Cyg (Hayes 1985; Lupie & Nordsieck 1987; Taylor et al. 1991; Nordsieck et al. 2001; Davies et al. 2005), and numerous SMC/LMC LBVS (Davies et al. 2005). Schulte-Ladbeck et al. (1993) suggested a link between the geometry of the present-day wind in R127, diagnosed via polarimetric observations, and the geometry of an older eruption which created a shell. Linking previous large mass-loss events with current stellar activity can provide important constraints for efforts to understand the physics behind massive LBV eruptions.

We have been monitoring the candidate LBV MWC 314 spectropolarimetrically for 6 years and spectroscopically for 4 years in an effort to diagnose its circumstellar environment and compare its properties with those of known LBVs. In Section 2, we summarize the acquisition and reduction of these data. The spectroscopic variability of MWC 314 is detailed in Section 3.1 and the variability of its total polarization is outlined in Section 3.2. In Section 3.3, we discuss our efforts to identify the interstellar polarization along the line of sight to MWC 314, while Section 3.4 describes the intrinsic polarization component which results after the interstellar component has been removed. A discussion of the implications of these

data is presented in Section 4.

2. Observations

MWC 314 was monitored from August 1999 through September 2004 with the HPOL spectropolarimeter, mounted on the 0.9m telescope at the University of Wisconsin's Pine Bluff Observatory (PBO). Sixteen observations were made using the red grating, providing spectropolarimetric coverage from ∼6000-10500 Å at a resolution of ∼10 Å (Nordsieck & Harris 1996), and were recorded with a 400 x 1200 pixel CCD camera. MWC 314 was observed using a 6 arc-second slit aligned E-W and a 200 arc-second decker aligned N-S on the sky. Data were processed using UW's REDUCE software package(Wolff et al. 1996): further information regarding HPOL and REDUCE are detailed in Nook (1990) and Harries et al. (2000).

The instrumental polarization of HPOL has been monitored on an approximately monthly basis since HPOL's inception in 1989 via observations of polarized and unpolarized standard stars. Our data have been corrected for such instrumental effects to an absolute accuracy of 0.025% and 1° in the R band. As noted in Harries et al. (2000), HPOL spectroscopic data are not calibrated to an absolute flux level due to the variable sky conditions routinely present.

Additional spectroscopic observations of MWC 314 were obtained with the 1-m RCC telescope of the Assy-Turgen high-altitude Observatory of the Fesenkov Astrophysical Institute (FAI) (Kazakhstan). Spectra covering the wavelength regime 6500-6700 Å were acquired with a standard UAGS spectrograph and a 1530 x 1020 ST-8Ei CCD camera with pixels 9 x 9 mm in size. The reciprocal dispersion of the instrument is 0.5 Å mm^{-1}. A 3 arc-second slit (3-pixel wide) was used for the observations. For flat-fielding, reflection spectra of the telescope dome illuminated by an ordinary tungsten-filament light bulb were recorded. The spectra were not corrected for the instrumental profile function. The Hα equivalent widths (EWs) were measured with no correction for the atmospheric absorption spectrum.

3. Results

3.1. Spectroscopy

Table 1 summarizes the observational data which are analyzed in this study. Miroshnichenko et al. (1998) used high-resolution spectroscopy to document the wealth of optical

emission lines which MWC 314 exhibits; however, they did not detect evidence of variability in their limited dataset. To search for evidence of Hα variability, we measured the Hα EWs of our dataset. For our spectropolarimetric dataset, the spectral regions spanning 6300-6400 Å and 6720-6820 Å were used to measure the continuum flux level around Hα, while the region ∼6518-6622 Å was used to determine the Hα line flux. A limited number of our observations suffered from less than perfect wavelength calibration: we took great care to ensure our measurements of line flux always probed the same spectral region in every observation. Our FAI spectra covered the region 6500-6700 Å. Data were continuum normalized using line-free regions in this spectral range, and EWs were systematically determined using standard IRAF techniques.

We tabulate our EW measurements in Table 1 and plot their time dependence in Figure 1. Our FAI EWs appear to be systematically larger than those derived from our PBO spectropolarimetric dataset by ∼28 Å. We believe that the wings of the Hα emission in MWC 314 are not fully contained within the spectral bandpass of the FAI data, leading to improper continuum normalization and hence the systematic inflation of measured EWs. We have recorded the actual measured EWs for our FAI data in Table 1, and have applied a -28 Å shift to these data in Figure 1. Errors associated with our equivalent width measurements are dominated by continuum placement uncertainty, which we estimate contributes an uncertainty of $< 5\%$ to all measurements; photon statistics errors are less than 1 Å.

Inspection of Table 1 and Figure 1 shows that the Hα EW often is seen at a level of 142 Å, consistent with that measured by Miroshnichenko (1996) and Miroshnichenko et al. (1998). Contrasting these earlier observations, our data show distinct deviations from this average EW, with emission strengths varying from 115 Å to 149 Å. We observe no periodicity in this changing emission strength, although our sparse sampling likely masks the presence of any true periodic behavior inherent in our data. Interestingly, our FAI spectra, which were obtained at a higher sampling frequency than our PBO data, exhibits substantial variability on timescales of several days to weeks. We encourage future moderate resolution spectroscopic monitoring with a higher sampling frequency to search for both evidence of binarity and detailed line profile variability.

3.2. Total Polarization Variability

It is well established that the polarized light we observe from astronomical sources can be comprised of two distinct components: an intrinsic polarization component originating at a source or its immediate vicinity and an interstellar polarization (ISP) component created by the dichroic absorption of starlight along a line of sight by aligned dust grains. For

unresolved sources such as MWC 314, an intrinsic polarization component will be observed if either the source has an asymmetrical circumstellar geometry or the illumination source of a symmetrical circumstellar envelope is time-dependent (Bjorkman 2000). Conversely, one would not expect the ISP along a line of sight to vary; hence, observing variability in the total polarization of an object is equivalent to detecting the presence of an intrinsic polarization component.

To better visualize any polarimetric variability present in our data, we have binned, i.e. reduced the resolution of our data to a standard Johnson R filter, as seen in Figure 1 and tabulated in Table 1. These broadband polarization measurements clearly exhibit a significant time-dependent behavior, with R-band polarizations ranging from 2.21% to 3.00% at position angles consistently around 0°. Thus MWC 314 must possess a variable intrinsic polarization component. There does not appear to be any firm correlation between the time variability of the total R band polarization and the Hα EW.

Figures 2 presents the total polarization of each of our observations, after the data was binned to a constant error level. Although not pictured here, the polarization position angle of these data exhibited a near constant, wavelength independent value of $\sim$179°. A dashed vertical line through these Figures denotes the wavelength of Hα. Note that quite a few of our observations show distinct polarization features at Hα, namely depolarization effects. In Section 3.3 we will discuss how this depolarization phenomenon can be used as a tool to constrain the ISP component along the line of sight.

3.3. Interstellar Polarization

Because polarization components add vectorally, it is possible to isolate and study the behavior of intrinsic polarization signatures of stars if their ISP components are accurately identified. Numerous techniques have been established for removing ISP, as detailed by McLean & Clarke (1979), Quirrenbach et al. (1997), and Bjorkman et al. (2006). Each technique has its limitations, some of which we now review.

A traditional way of determining foreground ISP is via field star studies. If one can locate a sample of stars which a) are within a small angular separation from and at the same general distance to the target object, such that every star's light will pass through the same interstellar medium conditions and b) exhibit no intrinsic polarization, then the averaged polarization of these field stars provides an estimate of the ISP along the particular line of sight. Miroshnichenko et al. (1998) determined a distance to MWC 314 of 3.0 $\pm$ 0.2 kpc: searches of polarization catalogs such as Heiles (2000) do not show any suitable field stars

which meet the aforementioned requirements. HD 174571 is a small angular distance away from MWC 314 and we estimate its distance to be ∼0.5 kpc based upon its brightness and reddening (Vieira et al. 2003); however, it is classified as a Be star and thus likely has a variable intrinsic polarization component. HD 183143, a suggested polarization standard star which has been observed to be variable at a level of 0.3% (Hsu & Breger 1982), is also located at a small angular distance from MWC 314. Based upon its distance, ∼1.6 kpc from its brightness and reddening, HD 183143 shows an enormous interstellar polarization of ∼6.0% at a PA of ∼0° in V, which Schultz & Lenzen (1983) notes differs greatly from the typical ISP value of 1-3% at a PA of ∼60° found in that region (Mathewson & Ford 1970). It thus seems likely that the interstellar medium near MWC 314's line of sight is quite complex, implying that the field star technique is not an appropriate tool for determining MWC 314's ISP.

Another technique often employed to determine ISP components is to measure the polarization across intrinsically unpolarized emission lines. Such a technique makes the assumption that most recombination events occur outside of the innermost circumstellar region which polarizes light (Harrington & Collins 1968). Polarization can simply be viewed as the ratio of scattered to total (scattered plus unscattered) intensity. The influx of a large number of unpolarized Hα line photons will significantly dilute the presence of any polarized continuum photons, causing the emission line to appear "depolarized". Thus the polarization measured across emission lines should be purely interstellar in origin. Such an assumption is not always fully accurate (McLean & Clarke 1979; Quirrenbach et al. 1997); however, the technique has been used to provide ISP estimates in previous studies of LBVs (Taylor et al. 1991; Schulte-Ladbeck et al. 1993, 1994; Nordsieck et al. 2001). Inspection of Figure 2 indeed shows that most of our observations exhibit Hα depolarization effects. We measured the Hα and continuum polarization for each of our observations, using the continuum bandpass definition discussed in Section 3.1 and a 50 Å bandpass, centered on Hα, to sample the core of the Hα line. The results are plotted on a Stokes Q-U diagram in Figure 3, where solid symbols correspond to line polarizations, open symbols represent continuum polarizations, and error bars correspond to 1-σ photon statistics errors. Solid lines connect the line and continuum polarization for each observation. Most of these lines point to one specific area in the Q-U diagram, i.e. the likely ISP for MWC 314. With the exception of the 4 vectors which do not point to this common area, specifically data from 6 August 1999, 8 August 2002, 3 September 2003, and 3 June 2004, we averaged all line polarizations together using a $1/\sigma^2$ weighting technique. The resulting Stokes parameters, Q = 2.59% and U = -0.14% (P = 2.59% PA = 179°), define our estimate of the ISP at 6563 Å. In Section 4, we will further discuss the implications of excluding the 4 aforementioned nights in this determination of MWC 314's ISP.

We can parameterize the ISP using the empirical Serkowski law(Serkowski et al. 1975), as modified by Wilking et al. (1982),

$$P_\lambda = P_{max} \times exp[-K \times ln^2(\lambda_{max}/\lambda)], \quad (1)$$

where P_{max} is the maximum polarization and λ_{max} is the wavelength at which P_{max} occurs. Assuming a typical value of λ_{max}, 5500 Å, and our measured ISP at Hα, we determine P_{max} to be 2.67%. In summary, our ISP parameters are $P_{max} = 2.67\%$, $\lambda_{max} = 5500$ Å, $\theta = 179°$, and K = 0.923.

3.4. Intrinsic Polarization Variability

Using the ISP parameters discussed in Section 3.3, we removed the interstellar polarization from our data. To check the accuracy of this process, we measured the intrinsic polarization of Hα and its surrounding continuum for our data using the same bandpass definitions discussed in Section 3.3. We plot the results on a Stokes Q-U diagram, seen in Figure 4, where closed symbols again represent Hα line polarization and open symbols represent continuum polarization measurements. With the exception of the 4 previously identified anomalous observations, all Hα line polarizations congregate around the origin as expected if these lines exhibit only ISP. Interestingly, the line-to-continuum polarization data trace out radial patterns from the origin in random directions, indicating there exists no consistent position angle in the intrinsic polarization.

Figures 5 and 6 illustrate the wavelength dependence of the intrinsic polarization of our data. The magnitude of the intrinsic polarization is clearly time dependent, with R-band polarizations varying from 0.09% to 0.58%. The intrinsic continuum polarization and position angle for each night are both generally wavelength independent, a signature of polarization arising from electron scattering with no subsequent attenuation. The polarization position angles fill all four quadrants of Stokes Q-U space, indicating there is no single scattering geometry present. Note that whenever polarization measurements approach zero their corresponding position angles are poorly constrained; hence, the large error bars present in some data plotted in Figure 5 and 6 should not be construed as excessively noisy data.

4. Discussion

Recall that we used the presence of depolarized emission lines in many of our observations to isolate and remove the ISP along the line of sight to MWC 314. In the process of determining this ISP component, we remarked that several observations showed abnormal

Hα line polarizations (e.g., Figure 3) and omitted these data from our ISP determinations. Using the polarization of emission lines as a basis for determining ISP parameters assumes that most recombination events occur outside of the region immediately surrounding a star which has a high free electron density, i.e. the polarizing region. If many Hα recombination photons do experience a scattering event in the polarizing region, then intrinsic Hα line polarization can arise. We suggest that the sporadic observations which show intrinsic Hα line polarization, specifically the 6 August 1999 (Figure 5) and 8 August 2002 (Figure 6) data, arise from density enhancements near the base of MWC 314's wind. We would expect that as these density clumps propagate away from and exit the polarizing region of the wind, the intrinsic polarization of Hα would decrease to its nominal "depolarized" state, e.g. transition to exhibiting zero intrinsic polarization.

The geometry of MWC 314's circumstellar envelope was previously explored by Miroshnichenko et al. (1998), who suggested the envelope was non-spherical and not viewed edge-on, based upon Balmer line profiles. Our data clearly illustrate that MWC 314 exhibits a time-dependent intrinsic polarization component, indicating the presence of an asymmetrical circumstellar envelope. The wavelength-independent nature of MWC 314's intrinsic polarization strongly suggests that electron scattering is the dominant polarizing mechanism. The position angle of this intrinsic polarization varies throughout all four quadrants of the Stokes Q-U plane, indicating that there is no preferred scattering plane, such a disk, in MWC 314's envelope. We note that the LBV P Cygni exhibits an intrinsic polarization whose position angle also varies significantly over time, which Taylor et al. (1991) and Nordsieck et al. (2001) interpreted as evidence of electron scattering in a clumpy wind (see Figure 10a of Taylor et al. 1991 for a graphical illustration). We have previously speculated that the sporadic observations of intrinsic Hα line polarization may be due to clumps near the base of MWC 314's wind; we also suggest that, like P Cygni, the general behavior of MWC 314's intrinsic polarization and position angle may be explained by electron scattering in an envelope characterized by density inhomogeneities, e.g. clumps. As the distribution and density of these clumps in the wind change over time, the globally averaged polarization position angle and magnitude will also fluctuate over the entire Q-U plane.

As detailed by Nota et al. (1995), the majority of LBVs exhibit some type of axisymmetric circumstellar geometry which likely influence the morphology of their ejected nebulae. Schulte-Ladbeck et al. (1993), for example, noted that the morphology of the LBV R137's nebula seemed to correspond to the circumstellar geometry derived from their polarimetric observations. The major exception to this basic geometry is P Cygni, which seems to exhibit a spherically symmetric nebula characterized by an asymmetrical distribution of clumps (Taylor et al. 1991; Barlow et al. 1994; Skinner et al. 1997). Our observations of MWC 314 do not reveal the presence of an axisymmetric circumstellar environment; rather, its envi-

ronment is more similar to that observed for P Cygni, i.e. an asymmetrical clumpy wind. We thus speculate that, like P Cygni, if MWC 314 undergoes an eruptive outburst in the near future, its morphology will be generally spherically symmetric and characterized by an asymmetrical distribution of density enhancements.

We suggest a number of followup observations which would further refine our understanding of MWC 314's circumstellar environment. Our spectroscopic observations showed clear signs of Hα variability, yet much better data sampling will be required to search for the short- and long-term periodic behavior common amongst many LBVs. Detailed information regarding the nature of the clumpy wind we detected can be derived from our data (e.g., Cassinelli et al. 1987; Taylor et al. 1991; Nordsieck et al. 2001) if we can refine the inclination of MWC 314's extended envelope. Searches for remnants of past eruption events, which may still exhibit diffuse radio or infrared emission, should also be attempted.

5. Summary

We have presented the results from a longterm spectroscopic and spectropolarimetric study of the candidate Luminous Blue Variable MWC 314. We have detected the first conclusive evidence of Hα equivalent width variability. The observed variability of MWC 314's total polarization indicates the presence of an intrinsic component, hence an asymmetrical circumstellar environment. Using depolarized Hα emission, we determined the ISP along the line of sight to MWC 314, allowing us to study its intrinsic component in detail. We find MWC 314's intrinsic polarization is wavelength independent and exhibits no single scattering geometry. We suggest that electron scattering off of a time variable distribution of density clumps in the wind is responsible for the behavior of this intrinsic polarization component. We find occasional evidence of intrinsic Hα line polarization and suggest such events are probing density enhancements at the base of MWC 314's wind. Finally, we note similarities between the polarimetric properties of MWC 314 and the LBV P Cygni, and suggest that any future eruptive outburst from MWC 314 may resemble the morphology exhibited by P Cygni.

We would like to thank Ken Nordsieck for providing access to the HPOL spectropolarimeter, and the PBO observing team for obtaining these data. We also thank the annonymous referee for providing helpful suggestions to improve this paper. This work has been supported in part by NASA LTSA grant NAG5-8054 (KSB, ASM) and NASA GSRP fellowship NGT5-50469 (JPW). K.S.B. is a Cottrell Scholar of the Research Corporation, and gratefully acknowledges their support. Partial support for HPOL has been provided by

NASA grant NAS5-26777. This research has made use of the SIMBAD database operated at CDS, Strasbourg, France, and the NASA ADS system.

REFERENCES

Barlow, M.J., Drew, J.E., Meaburn, J., & Massey, R.M. 1994, MNRAS, 268, L29

Bjorkman, K. 2000, in IAU Colloq. 175, The Be Phenomenon in Early-Type Stars, ed. M.A. Smith, H.F. Henrichs, & J. Fabregat (San Francisco: ASP), ASP Conf. Ser. 214, 384 in Early-Type Stars,

Bjorkman, K.S., Wisniewski, J.P., & Meade, M.R. 2006, in prep

Cassinelli, J.P., Nordsieck, K.H., & Murison, M.A. 1987, ApJ, 317, 290

Clampin, M., Schulte-Ladbeck, R.E., Nota, A., Robberto, M., Paresce, F., & Clayton, G.C. 1995, AJ, 110, 251

Davies, B., Oudmaijer, R.D., & Vink, J.S. 2005, A&A, 439, 1107

Harries, T.J., Babler, B.L., & Fox, G.K. 2000, A&A, 361, 273

Harrington, J.P. & Collins, G.W. II 1968, ApJ, 151, 1051

Hayes, D.P. 1985, ApJ, 289, 726

Heiles, C. 2000, AJ, 119, 923

Hsu, J.-C. & Breger, M. 1982, ApJ, 262, 732

Humphreys, R. & Davidson, K. 1994, PASP, 106, 1025

Leitherer, C., Allen, R., Altner, B., Damineli, A., Drissen, L., Idiart, T., Lupie, O., Nota, A., Robert, C., Schmutz, W., & Shore, S. 1994, ApJL, 428, 292

Lupie, O.L. & Nordsieck, K.H. 1987, AJ, 92, 214

Mathewson, D.S. & Ford, V.L. 1970, MmRAS, 74, 139

McLean, I.S. & Clarke, D. 1979, MNRAS, 186, 245

Miroshnichenko, A.S. 1996, A&A, 312, 941

Miroshnichenko, A.S., Fremat, Y., Houziaux, L., Andrillat, Y., Chentsov, E.L., & Klochkova, V.G. 1998, A&AS, 131, 469

Nook, M. 1990, Ph.D. dissertation, The University of Wisconsin-Madison

Nordsieck, K.H. & Harris, W. 1996, in ASP Conf. Ser. 97, Polarimetry of the Interstellar Medium, ed. W. G. Roberge & D. C. B. Whittet (San Francisco: ASP), 100

Nordsieck, K.H., Wisniewski, J.P., Babler, B.L., Meade, M.R., Anderson, C.M., Bjorkman, K.S., Code, A.D., Fox, G.K., Johnson, J.J., Weitenbeck, A.J., & Zellner, N.E.B 2001, in ASP Conf. Ser. 233, P Cygni 2000: 400 Years of Progress, ed. M. de Groot & C. Sterken (San Francisco: ASP), 261

Nota, A., Livia, M., Clampin, M., & Schulte-Ladbeck, R. 1995, ApJ, 448, 788

Parthasarathy, M., Jain, S.K., & Bhatt, H.C. 2000, A&A, 355, 221

Perryman, M.A.C. et al. 1997, A&A, 323, L49

Quirrenbach, A., Bjorkman, K.S., Bjorkman, J.E., Hummel, C.A., Buscher, D.F., Armstrong, J.T., Mozurkewich, D., Elias, N.M. II, & Babler, B.L. 1997, ApJ, 479, 477

Schultz, A. & Lenzen, R. 1983, A&A, 121, 158

Schulte-Ladbeck, R.E., Leitherer, C., Clayton, G.C., Robert, C., Meade, M.R., Drissen, L., Nota, A., & Schmutz, W. 1993, ApJ, 407, 723

Schulte-Ladbeck, R.E., Clayton, G.C., Hillier, D.J., Harries, T.J., & Howarth, I.D. 1994, ApJ, 429, 846

Schulte-Ladbeck, R.E., Pasquali, A., Clampin, M., Nota, A., Hillier, D.J., & Lupie, O.L. 1999, AJ, 118, 1320

Serkowski, K., Mathewson, D.S., & Ford, V.L. 1975, ApJ, 196, 261

Skinner, C.J., Exter, K.M., Barlow, M.J., Davis, R.J., & Bode, M.F. 1997, MNRAS, 288, L7

Taylor, M., Nordsieck, K.H., Schulte-Ladbeck, R.E., & Bjorkman, K.S. 1991, AJ, 102, 1197

van Genderen, A.M. 2001, A&A, 366, 508

Vieira, S.L.A., Corradi, W.J.B., Alencar, S.H.P., Mendes, L.T.S., Torres, C.A.O., Quast, G.R., Guimaraes, M.M., & da Silva, L. 2003, AJ, 126, 2971

Wilking, B.A., Lebofsky, M.J., & Rieke, G.H. 1982, AJ, 87, 695

Wolff, M.J., Nordsieck, K.H., & Nook, M.A. 1996, AJ, 111, 856

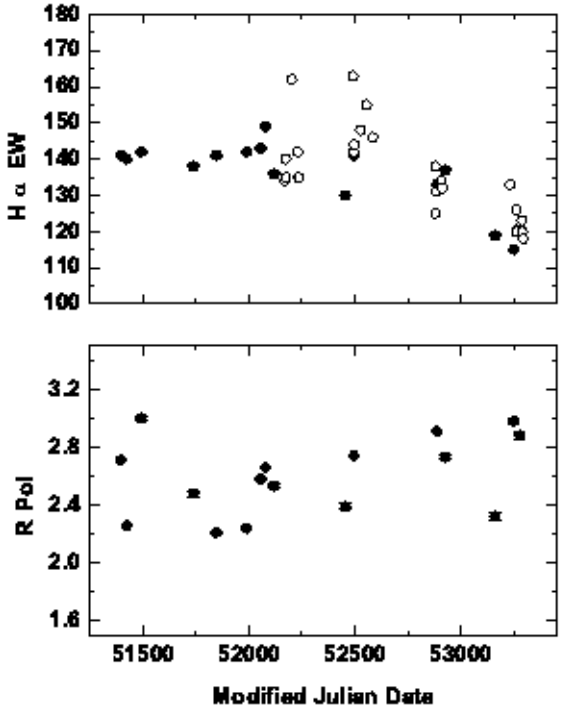

Fig. 1.— Hα equivalent widths and R band polarizations of MWC 314 are plotted as a function of time. Open circles correspond to FAI spectroscopic observations, which as discussed in the text have been shifted in magnitude by -28 Å. Filled circles correspond to HPOL spectropolarimetric data. The dominant source of error in these measurements is our choice of continuum placement; the photon statistic errors associated with these measurements are less than 1 Å. Note that the polarization error bars are often smaller than the size of the data points.

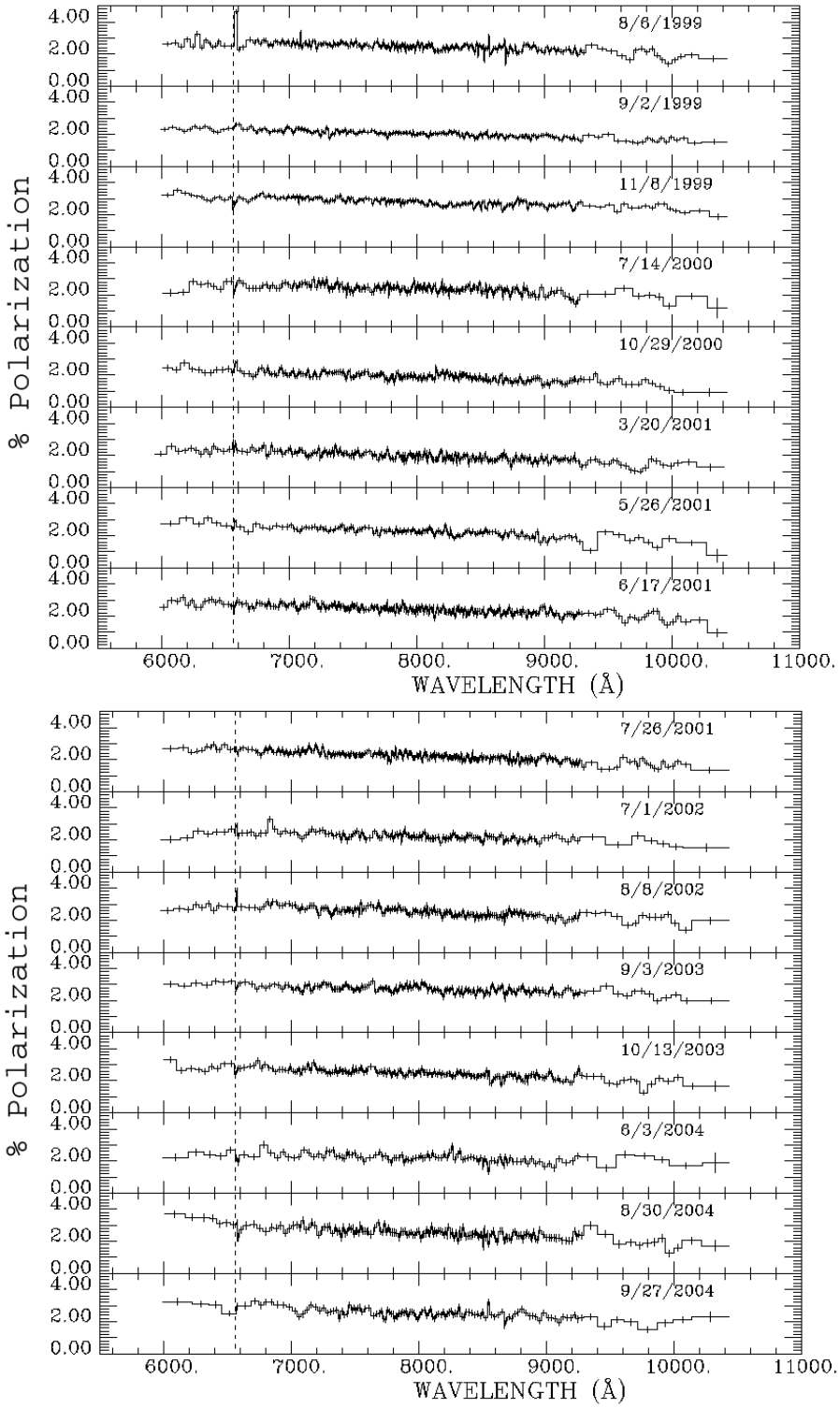

Fig. 2.— Time variability of MWC 314's total R band polarization. The dashed vertical line indicates the position of Hα.

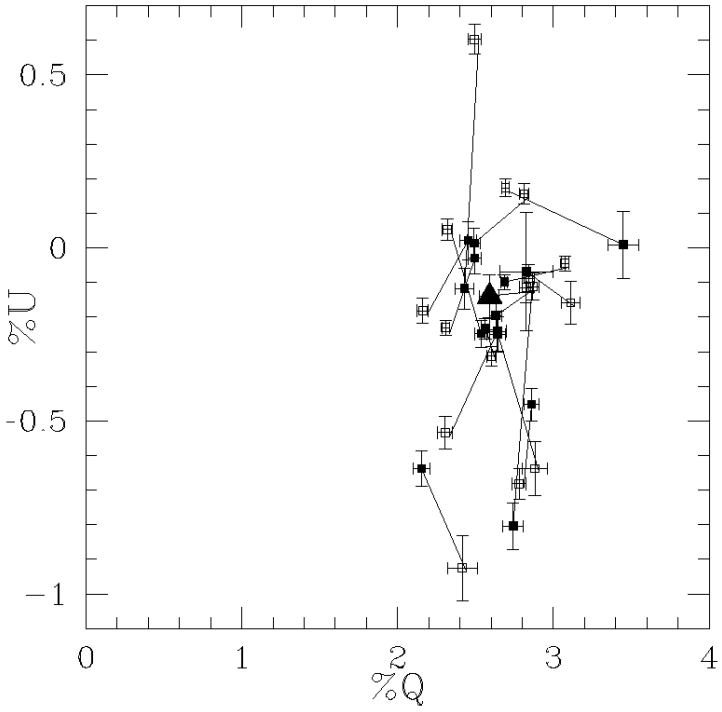

Fig. 3.— Q-U diagram of MWC 314's total polarization. Solid squares denote the polarization at Hα while open squares denote the continuum polarization. Note that most of the lines connecting an observation's continuum to Hα polarization point to one location in the Q-U diagram. Assuming Hα should generally be unpolarized, this location identifies the ISP along the line of sight. The ISP we calculated by averaging most of these Hα polarizations is given by the large, solid triangle, located at Q = 2.83% and U = -0.07%.

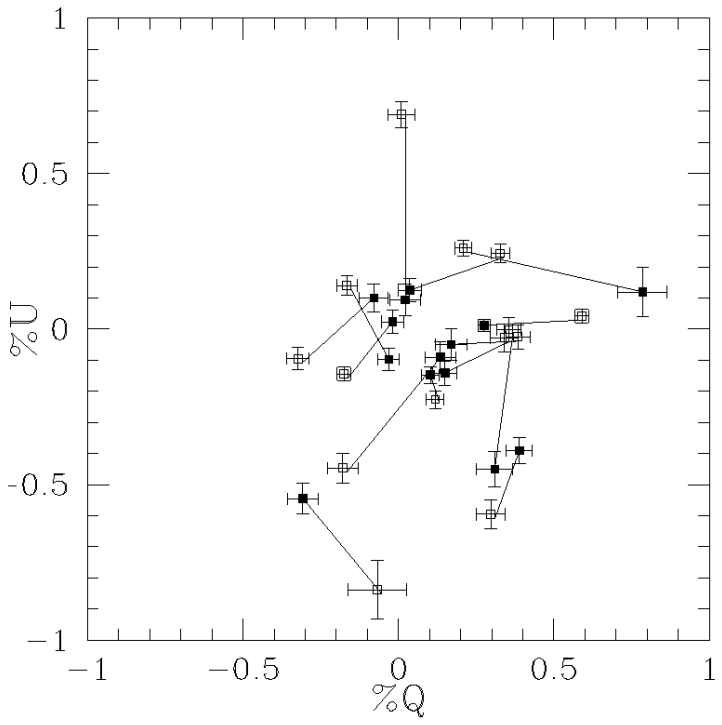

Fig. 4.— Q-U diagram of MWC 314's intrinsic polarization. Note that most of the Hα line polarizations, to within 3-σ, now fall near the origin. Such a scenario is expected if Hα is generally unpolarized. The lines connecting each observation's line to continuum polarization are oriented randomly about the origin, indicating that there is no single preferred position angle to the intrinsic polarization component.

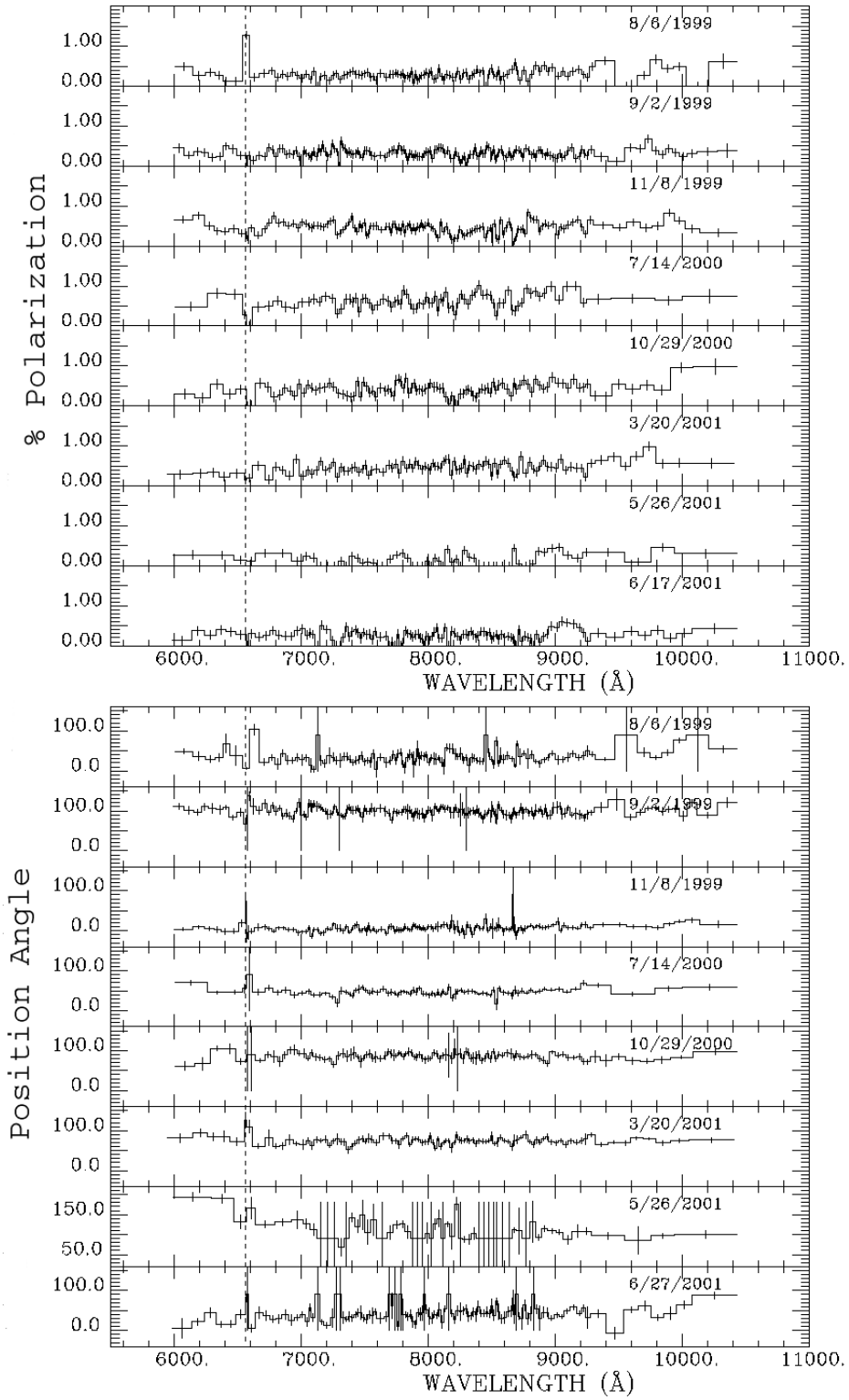

Fig. 5.— Time variability of MWC 314's total R band intrinsic polarization and position angle for the first half of our dataset. The dashed vertical line indicates the position of Hα. Note that the polarization and position angle for each observation are generally wavelength-independent, indicating electron scattering is the dominant polarizing mechanism.

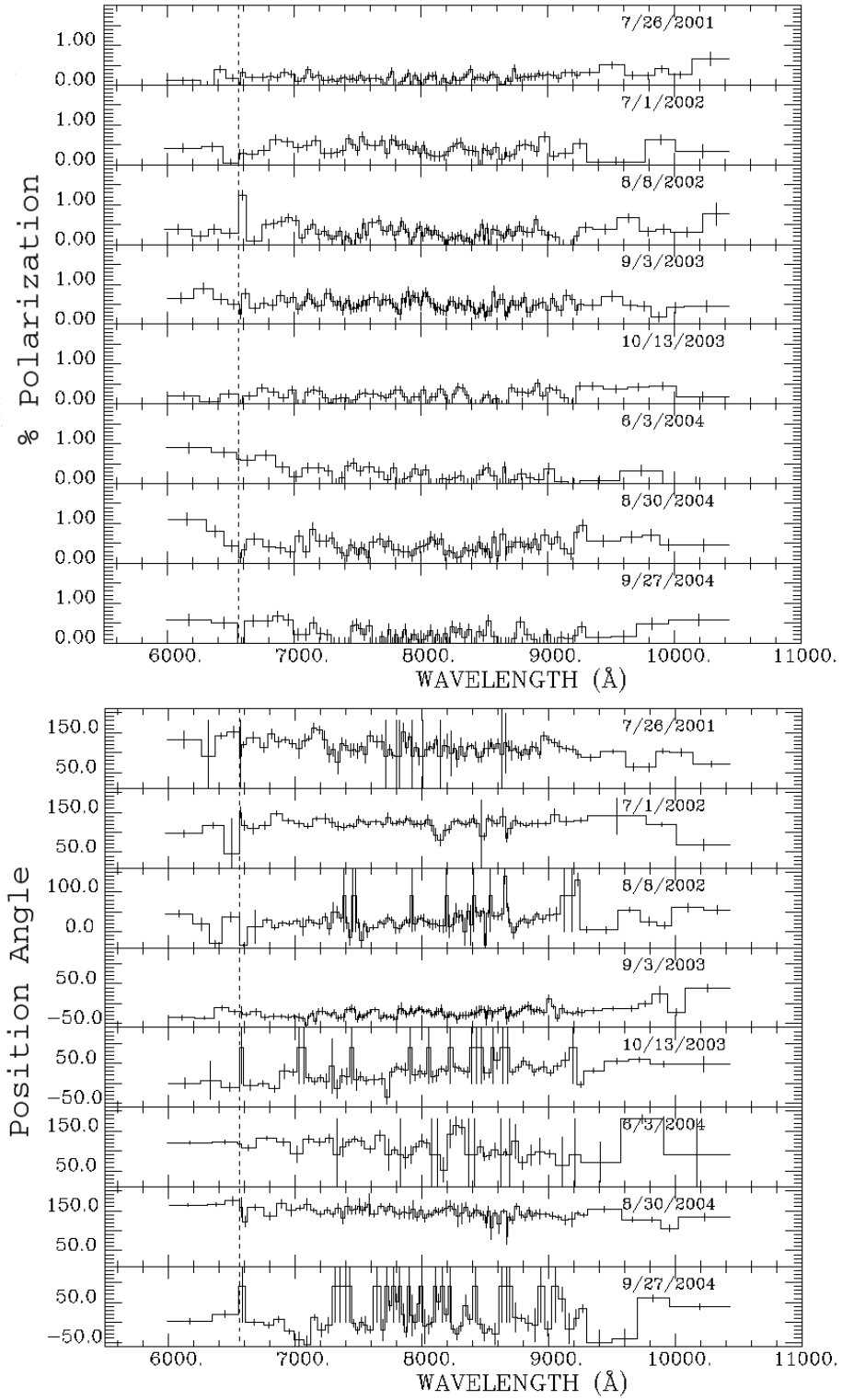

Fig. 6.— Time variability of MWC 314's total R band intrinsic polarization and position angle for the second half of our dataset. The dashed vertical line indicates the position of Hα. Note that the polarization and position angle for each observation are generally wavelength-independent, indicating electron scattering is the dominant polarizing mechanism.

Table 1:

Date	MJD	Location	Hα EW	%Pol$_R$	PA$_R$
8-6-1999	51397	P	141	2.71 ± 0.01%	1
9-2-1999	51424	P	140	2.26 ± 0.01%	178
11-8-1999	51491	P	142	3.00 ± 0.01%	0
7-14-2000	51740	P	138	2.48 ± 0.02%	5
10-29-2000	51847	P	141	2.21 ± 0.01%	0
3-20-2001	51989	P	142	2.24 ± 0.01%	1
5-26-2001	52056	P	143	2.58 ± 0.01%	178
6-17-2001	52078	P	149	2.66 ± 0.01%	1
7-26-2001	52117	P	136	2.53 ± 0.01%	177
9-16-2001	52169	F	162	···	···
9-20-2001	52173	F	163	···	···
9-21-2001	52174	F	168	···	···
10-18-2001	52201	F	190	···	···
11-16-2001	52230	F	170	···	···
11-18-2001	52232	F	163	···	···
11-21-2001	52235	F	163	···	···
7-1-2002	52457	P	130	2.39 ± 0.02%	175
8-5-2002	52492	F	191	···	···
8-6-2002	52493	F	170	···	···
8-8-2002	52495	P	141	2.74 ± 0.01%	0
8-9-2002	52496	F	172	···	···
9-7-2002	52525	F	176	···	···
10-9-2002	52556	F	183	···	···
11-6-2002	52585	F	174	···	···
8-28-2003	52880	F	153	···	···
8-29-2003	52881	F	166	···	···
8-31-2003	52883	F	159	···	···
9-3-2003	52886	P	133	2.91 ± 0.01%	174
9-25-2003	52908	F	162	···	···
9-29-2003	52912	F	160	···	···
10-13-2003	52926	P	137	2.73 ± 0.01%	0
6-3-2004	53160	P	119	2.32 ± 0.02%	173
8-13-2004	53231	F	161	···	···
8-30-2004	53248	P	115	2.98 ± 0.02%	175
9-12-2004	53261	F	148	···	···
9-13-2004	53262	F	154	···	···
9-27-2004	53276	P	121	2.88 ± 0.03%	179
10-8-2004	53288	F	151	···	···
10-11-2004	53290	F	148	···	···
10-14-2004	53293	F	146	···	···

Note. — Summary of MWC 314 observations. The date is tabulated according to MM-DD-YYYY and MJD is an abbreviation for the modified Julian date of the observation. Data obtained at Pine Bluff Observatory is labeled with a "P" in column 3, while data obtained at the Fesenkov Astrophysical Institute is labeled with a "F" in column 3. Also listed is the Hα equivalent width (EW), with positive values corresponding to emission, the raw polarization in the R filter, and the raw position angle (PA) in the R filter. As described in the text, our FAI EWs appear to be systematically $\sim$28Ålarger than those derived from our PBO data.